

# Exergy-based ecological optimization for an endoreversible variable-temperature heat reservoir air heat pump cycle

Yuehong Bi<sup>a,b</sup>, Lingen Chen<sup>b,\*</sup>, and Fengrui Sun<sup>b</sup>

<sup>a</sup>*Institute of Civil & Architectural Engineering,*

*Beijing University of Technology, Beijing 100124, P.R. China,*

<sup>b</sup>*Postgraduate School, Naval University of Engineering, Wuhan 430033, P.R. China,*

*Tel: 0086-27-83615046; Fax: 0086-27-83638709*

*\*e-mail: lgchenna@yahoo.com; lingchen@hotmail.com*

Recibido el 1 de diciembre de 2008; aceptado el 20 de enero de 2009

An ecological performance analysis and optimization based on the exergetic analysis is carried out in this paper for an endoreversible air heat pump cycle with variable-temperature heat reservoirs. An exergy-based ecological optimization criterion, which consists of maximizing a function representing the best compromise between the exergy output rate and exergy loss rate (entropy generation rate and environment temperature product) of the heat pump cycle, is taken as the objective function. The analytical relation of the exergy-based ecological function is derived. The effects of pressure ratio, the effectiveness of the heat exchangers, the inlet temperature ratio of the heat reservoirs and the ratio of hot-side heat reservoir inlet temperature to ambient temperature on ecological function are analyzed. The cycle performance optimizations are performed by searching the optimum distribution of heat conductance of the hot- and cold-side heat exchangers for fixed total heat exchanger inventory and the optimum heat capacity rate matching between the working fluid and the heat reservoirs, respectively. The influences of some design parameters, including heat exchanger inventory and heat capacity rate of the working fluid on the optimal performance of the endoreversible air heat pump are provided by numerical examples. The results show that the exergy-based ecological optimization is an important and effective criterion for the evaluation of air heat pumps.

**Keywords:** Exergy-based ecological function; endoreversible air heat pump; variable-temperature heat reservoir; finite time thermodynamics.

Un análisis y una optimización ecológicos de funcionamiento basados en el análisis exergetic se realiza en este papel para un ciclo endoreversible de la bomba de calor del aire con los depósitos del calor de la variable-temperatura. Un criterio ecológico exergy-basado de la optimización, que consiste en el maximizar de una función que representa el mejor compromiso entre el índice de salida del exergy y el índice de la pérdida del exergy (producto de la temperatura de la tarifa y del ambiente de la generación de la entropía) del ciclo de la bomba de calor, se toma como la función objetiva. La relación analítica de la función ecológica exergy-basada se deriva. Los efectos del cociente de la presión, de la eficacia de los cambiadores de calor, del cociente de la temperatura de la entrada de los depósitos del calor y del cociente de la temperatura de la entrada del depósito del calor del caliente-lado a la temperatura ambiente en la función ecológica se analizan. Las optimizaciones del funcionamiento del ciclo son realizadas buscando la distribución óptima de la conductancia del calor de los cambiadores calientes y del frío-lado de calor para el inventario total fijo del cambiador de calor y la tarifa óptima de la capacidad de calor que empareja entre el líquido de funcionamiento y los depósitos del calor, respectivamente. Las influencias de algunos parámetros de diseño, incluyendo inventario del cambiador de calor y el índice de capacidad de calor del líquido de funcionamiento en el funcionamiento óptimo de la bomba de calor endoreversible del aire son proporcionadas por ejemplos numéricos. Los resultados demuestran que la optimización ecológica exergy-basada es un criterio importante y eficaz para la evaluación de las bombas de calor del aire.

**Descriptores:** Función ecológica exergy-basada; bomba de calor endoreversible del aire; depósito del calor de la variable-temperatura; termodinámica de tiempo finitas.

PACS: 01.40G; 05.70.-a; 64.70.F

## 1. Introduction

The environmental problems (ozone layer damage, global warming) associated with using HCFC and HFC refrigerants have spurred interest in alternative, natural refrigerants that can deliver safe and sustainable heat pump in the future. Air as refrigerant in an air heat pump cycle meets all criteria for a refrigerant being environmental friendly. Therefore, air heat pump is one of the most promising long-term survivors and the analysis for the air heat pump cycle has been paid more attentions [1-3].

Finite time thermodynamics (FTT) has become the premier method of thermodynamic analysis in thermodynamic

cycles and processes since the 1970s and now it is sweeping every aspect of physical and engineering practice [4-18]. The results obtained for various thermodynamic cycle analyses using FTT are closer to real device performance than those obtained using classical thermodynamics. FTT analysis for the performances of air heat pumps have been performed by some authors [19-24] for heating load, coefficient of performance (COP) [19-24] and heating load density (the ratio of heating load to the maximum specific volume in the cycle) [24] objectives.

In recent years, the research combining classic exergy concept [25-28] with FTT [4-18] is becoming increasingly important. The aspect that distinguishes FTT from pure ex-

ergy analysis is the minimization of the calculated entropy generation rate. At this point, Angulo-Brown *et al.* [29] proposed an ecological criterion  $\dot{E}' = \dot{P} - T_L\sigma$  for finite-time Carnot heat engines, where  $T_L$  is temperature of the cold reservoir,  $\dot{P}$  is the power output and  $\sigma$  is the entropy-generation rate. Yan [30] showed that it might be more reasonable to use  $\dot{E} = \dot{P} - T_0\sigma$  if the cold-reservoir temperature  $T_L$  is not equal to the environment temperature  $T_0$  because in the definition of  $\dot{E}'$ , two different quantity, exergy output  $\dot{P}$  and non-exergy  $T_L\sigma$ , were compared together. The optimization of the ecological function represents a compromise between the power output  $\dot{P}$  and the lost power  $T_0\sigma$ , which is produced by entropy generation in the system and its surroundings.

Based on the view of point of exergy analysis, Chen *et al.* [31] provided a unified ecological optimization objective for all of thermodynamic cycles including heat engine cycles, refrigeration cycles and heat pump cycles, that is

$$\dot{E} = \frac{A}{\tau} - T_0 \frac{\Delta S}{\tau} = \frac{A}{\tau} - T_0\sigma \quad (1)$$

where  $A$  is the exergy output of the cycle,  $T_0$  is the environment temperature of the cycle,  $\Delta S$  is the entropy generation of the cycle,  $\tau$  is the cycle period, and  $\sigma$  is the entropy generation rate of the cycle. Equation (1) represents the best compromise between the exergy output rate and the exergy loss rate (*i.e.* entropy generation rate) of the thermodynamic cycles. The ecological optimal performances of endoreversible and irreversible Carnot [32-34] and Stirling and Ericsson [35] heat-pump cycles were investigated.

In this paper, the optimal exergy-based ecological performance of an variable-temperature endoreversible air heat pump is derived by taking an ecological optimization criterion Eq. (4) as the objective. Numerical examples are given to show the effects of heat capacity rate of the working fluid

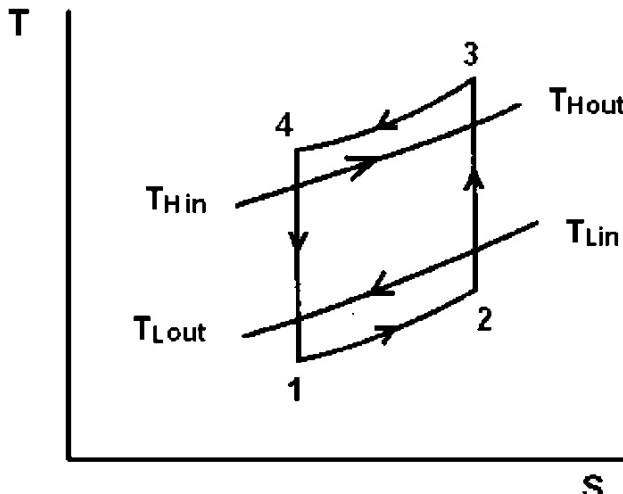


FIGURE 1. Temperature-entropy diagram of an endoreversible air heat pump cycle with variable-temperature heat reservoirs.

and heat exchanger inventory on the optimal performance of the variable-temperature endoreversible air heat pump.

## 2. Variable-temperature endoreversible air heat pump model

For heat pump cycles, the exergy output rate of the cycle is

$$\frac{A}{\tau} = \dot{Q}_H \left( 1 - \frac{T_0}{T_H} \right) - \dot{Q}_L \left( 1 - \frac{T_0}{T_L} \right) \quad (2)$$

where  $\dot{Q}_L$  is the rate of heat transfer supplied by the heat source,  $\dot{Q}_H$  is the rate of heat transfer released to the heat sink (*i.e.* the heating load), and  $T_H$  and  $T_L$  are temperatures of the heat sink and heat source, respectively.

The coefficient of performance (COP) of the heat pump cycle is

$$\beta = \frac{\dot{Q}_H}{(\dot{Q}_H - \dot{Q}_L)} \quad (3)$$

Substituting Eqs. (2) and (3) into Eq. (1) yields the ecological function of a heat pump cycle:

$$\dot{E} = \dot{Q}_H \left[ \left( 1 - \frac{T_0}{T_H} \right) - (1 - \beta^{-1}) \left( 1 - \frac{T_0}{T_L} \right) \right] - T_0\sigma \quad (4)$$

An endoreversible air heat pump cycle with variable-temperature heat reservoirs is shown in Fig. 1. The following assumptions are made for this model:

- (i) The working fluid flows through the system in a steady-state fashion. The cycle is a Brayton heat pump one which consists of two isobaric processes (1-2, 3-4) and two adiabatic processes (2-3, 4-1).
- (ii) The high-temperature (hot-side) heat sink is considered as having a finite thermal capacitance rate  $C_H$ . The inlet and outlet temperatures of the cooling fluid are  $T_{Hin}$  and  $T_{Hout}$ , respectively. The low-temperature (cold-side) heat source is considered as having a finite thermal capacitance rate  $C_L$ . The inlet and outlet temperatures of the heating fluid are  $T_{Lin}$  and  $T_{Lout}$ , respectively.
- (iii) The hot- and cold-side heat exchangers are considered to be counter-flow heat exchangers, and their heat conductance (heat transfer coefficient-area product) are  $U_H$  and  $U_L$ , respectively. The working fluid is an ideal gas having constant thermal capacitance rate (the product of mass flow rate and specific heat)  $C_{wf}$ .

The rate of heat transfer ( $\dot{Q}_H$ ) released to the heat sink, *i.e.* the heating load, and the rate of heat transfer ( $\dot{Q}_L$ ) supplied by the heat source, are given by, respectively

$$\dot{Q}_H = \frac{U_H[(T_3 - T_{Hout}) - (T_4 - T_{Hin})]}{\ln \left[ \frac{(T_3 - T_{Hout})}{(T_4 - T_{Hin})} \right]} = C_H(T_{Hout} - T_{Hin}) = C_{H\min} I_{H1}(T_3 - T_{Hin}) = C_{wf}(T_3 - T_4) \quad (5)$$

$$\dot{Q}_L = \frac{U_L[(T_{Lin} - T_2) - (T_{Lout} - T_1)]}{\ln \left[ \frac{(T_{Lin} - T_2)}{(T_{Lout} - T_1)} \right]} = C_L(T_{Lin} - T_{Lout}) = C_{L\min} I_{L1}(T_{Lin} - T_1) = C_{wf}(T_2 - T_1) \quad (6)$$

where  $U$  is the heat conductance,  $I_{H1}$  and  $I_{L1}$  are the effectivenesses of the hot- and cold-side heat exchangers, respectively, and  $N$  is the number of heat transfer units. They are defined as:

$$I_{H1} = \frac{1 - \exp \left[ -N_{H1} \left( 1 - \frac{(C_{H\min})}{(C_{H\max})} \right) \right]}{\left( 1 - \frac{C_{H\min}}{C_{H\max}} \right) \exp \left[ -N_{H1} \left( 1 - \frac{C_{H\min}}{C_{H\max}} \right) \right]} \quad (7)$$

$$I_{L1} = \frac{\left\{ 1 - \exp \left[ -N_{L1} \left( 1 - \frac{C_{L\min}}{C_{L\max}} \right) \right] \right\}}{\left\{ 1 - \left( \frac{C_{L\min}}{C_{L\max}} \right) \exp \left[ -N_{L1} \left( 1 - \frac{C_{L\min}}{C_{L\max}} \right) \right] \right\}} \quad (8)$$

where  $C_{H\min}$  and  $C_{H\max}$  are the minimum and maximum of  $C_H$  and  $C_{wf}$ , respectively, and  $C_{L\min}$  and  $C_{L\max}$  are the minimum and maximum of  $C_L$  and  $C_{wf}$ , respectively:

$$N_{H1} = \frac{U_H}{C_{H\min}}, \quad N_{L1} = \frac{U_L}{C_{L\min}}$$

$$C_{H\min} = \min\{C_H, C_{wf}\}, \quad C_{H\max} = \max\{C_H, C_{wf}\}$$

$$C_{L\min} = \min\{C_L, C_{wf}\}, \quad C_{L\max} = \max\{C_L, C_{wf}\} \quad (9)$$

The second law of thermodynamics requires  $T_1 T_3 = T_2 T_4$ . Combining Eqs. (5)-(9) gives:

$$T_3 = \frac{C_{wf} C_{L\min} I_{L1} T_{Lin} x + C_{H\min} I_{H1} T_{Hin} (C_{wf} - C_{L\min} I_{L1})}{C_{wf}^2 - (C_{wf} - C_{H\min} I_{H1})(C_{wf} - C_{L\min} I_{L1})} \quad (10)$$

$$T_4 = \frac{C_{wf} C_{H\min} I_{H1} T_{Hin} + C_{L\min} I_{L1} T_{Lin} (C_{wf} - C_{H\min} I_{H1}) x}{C_{wf}^2 - (C_{wf} - C_{H\min} I_{H1})(C_{wf} - C_{L\min} I_{L1})} \quad (11)$$

where  $x$  is the isentropic temperature ratio of the working fluid, that is,  $x = T_3/T_2 = (P_3/P_2)^m = P_r^m$ , where  $P_r$  is the pressure ratio of the compressor,  $n = (k - 1)/k$ , and  $k$  is the ratio of specific heats. Combining Eqs. (3), (4), (5), (6), (10)

with (11) gives the heating load ( $\dot{Q}_H$ ), the COP ( $\beta$ ) and the entropy-generation rate ( $\sigma$ ) of the cycle:

$$\dot{Q}_H = \frac{C_H \min C_L \min I_{H1} I_{L1} (T_{Lin}x - T_{Hin})}{C_H \min I_{H1} + C_L \min I_{L1} - \frac{(C_H \min C_L \min I_{H1} I_{L1})}{(C_{wf})}} \quad (12)$$

$$\beta = (1 - \frac{1}{x})^{-1} = \frac{x}{(x - 1)} = \frac{P_r^m}{(P_r^m - 1)} \quad (13)$$

$$\begin{aligned} \sigma &= \frac{C_H \ln \{1 + C_H \min C_L \min I_{H1} I_{L1} (x/\tau_3 - 1)\}}{C_H \left( C_H \min I_{H1} + C_L \min I_{L1} - \frac{(C_H \min C_L \min I_{H1} I_{L1})}{(C_{wf})} \right)} \\ &+ \frac{C_L \ln [1 - C_H \min C_L \min I_{H1} I_{L1} (1 - \tau_3/x)]}{C_L \left( C_H \min I_{H1} + C_L \min I_{L1} - \frac{(C_H \min C_L \min I_{H1} I_{L1})}{(C_{wf})} \right)} \end{aligned} \quad (14)$$

Substituting Eqs. (12) and (13) into Eq. (4) yields the exergy-based ecological function:

$$\dot{E} = \frac{C_H \min C_L \min I_{H1} I_{L1} (T_{Lin} - T_{Hin}/P_r^m)(P_r^m - 1)}{C_H \min I_{H1} + C_L \min I_{L1} - \frac{(C_H \min C_L \min I_{H1} I_{L1})}{(C_{wf})}} - 2T_0\sigma \quad (15)$$

The dimensionless ecological function  $\bar{E}$  is given by

$$\bar{E} = \frac{\dot{E}}{(C_H T_{Hin})} = \frac{C_H \min C_L \min I_{H1} I_{L1} (1/\tau_3 - 1/P_r^m)(P_r^m - 1)}{C_H C_H \min I_{H1} + C_H C_L \min I_{L1} - \frac{(C_H C_H \min C_L \min I_{H1} I_{L1})}{(C_{wf})}} - \frac{2\sigma}{\tau_4 C_H} \quad (16)$$

where  $\tau_3 = T_{Hin}/T_{Lin}$  and  $\tau_4 = T_{Hin}/T_0$  are the inlet temperature ratio of the heat reservoirs and the ratio of hot-side heat reservoir inlet temperature to ambient temperature, respectively.

Equation (13) shows that the COP ( $\beta$ ) of the endoreversible air heat pump is only dependent on  $P_r$ . The optimization of the exergy-based ecological function ( $\dot{E}$ ) does not affect the COP for the fixed pressure ratio.

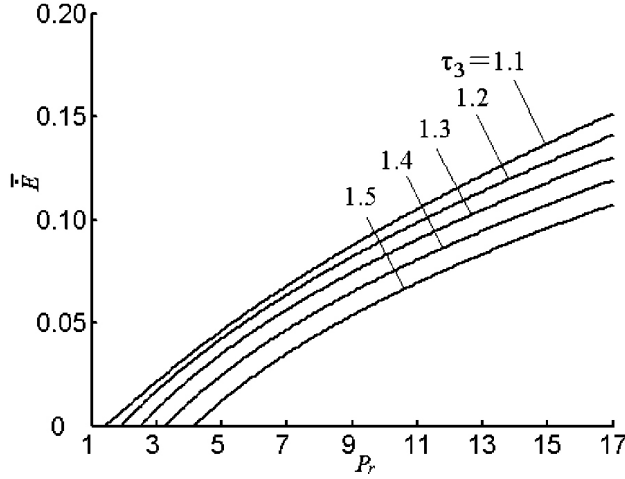


FIGURE 2. Dimensionless ecological function vs. pressure ratio.

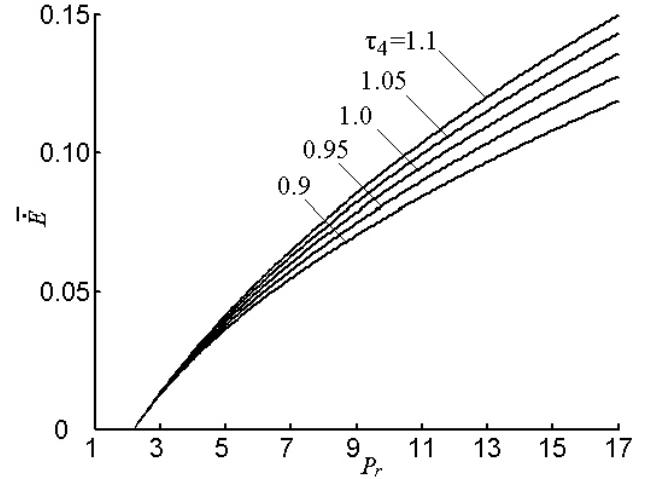


FIGURE 3. Effect of the ratio of hot-side heat reservoir inlet temperature to ambient temperature on the dimensionless ecological function vs. pressure ratio.

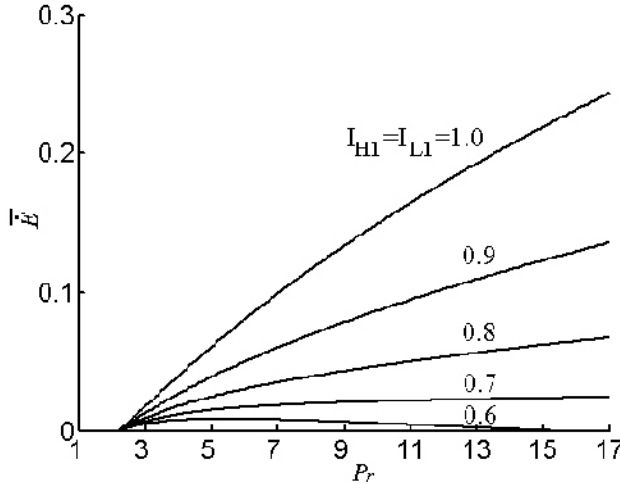


FIGURE 4. Effect of effectiveness of the heat exchangers on the dimensionless ecological function vs. pressure ratio.

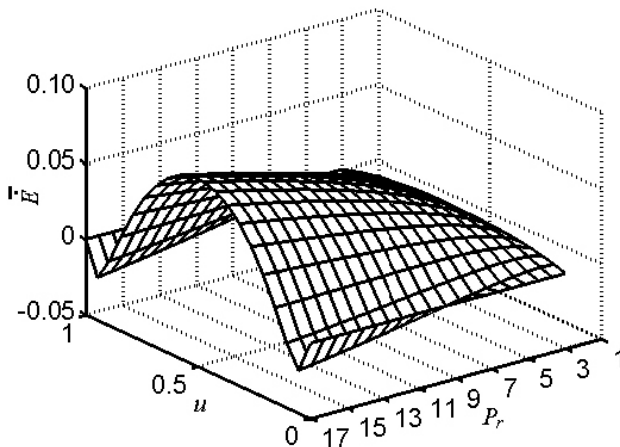


FIGURE 5. Comprehensive relationships among dimensionless ecological function, distribution of heat conductance and pressure ratio.

### 3. Analysis and Optimization

#### 3.1. Ecological function versus pressure ratio

Equation (16) shows that the dimensionless ecological function ( $\bar{E}$ ) is dependent on various design parameters. To see the effect of pressure ratio ( $P_r$ ) on the ecological function, detailed numerical examples are provided. The following data used in the numerical calculation come from the real example of Ref. 36, so that the analytical results can be validated. Figure 2 shows the relation of  $\bar{E}$  versus  $P_r$ . In the calculations,  $k=1.4$ ,  $\tau_4=1$ ,  $I_{H1}=I_{L1}=0.9$ ,

$C_L=C_H=1.0\text{kW}/K$  and  $C_{wf}=0.8\text{kW}/K$  are set. It indicates that the relation between  $\bar{E}$  and  $P_r$  is monotonically increasing function and  $\bar{E}$  decreases with the increase of inlet temperature ratio of the heat reservoirs ( $\tau_3$ ).

Figure 3 shows the effect of the ratio of hot-side heat reservoir inlet temperature to ambient temperature ( $\tau_4$ ) on  $\bar{E}$  versus  $P_r$  with  $k=1.4$ ,  $\tau_3=1.25$ ,  $I_{H1}=I_{L1}=0.9$ ,  $C_L=C_H=1.0\text{kW}/K$  and  $C_{wf}=0.8\text{kW}/K$ . It indicates that  $\bar{E}$  increase with the increase of the ratio of hot-side heat reservoir inlet temperature to ambient temperature ( $\tau_4$ ).

For the fixed total heat conductance of the hot- and cold-side heat exchangers, Fig. 4 shows the effect of heat exchanger effectiveness on  $\bar{E}$  versus  $P_r$  with  $k=1.4$ ,  $\tau_3=1.25$ ,  $\tau_4=1$ ,  $C_L=C_H=1.0\text{kW}/K$  and  $C_{wf}=0.8\text{kW}/K$ . It indicates that the heat exchanger effectiveness only affect quantitatively the dimensionless ecological function versus pressure ratio. It does not change the curve shape.  $\bar{E}$  increases with the increases in  $I_{H1}$  and  $I_{L1}$ .

#### 3.2. Optimal distribution of heat conductance

If the heat conductances of two heat exchangers are changeable, the dimensionless ecological function may be optimized by searching the optimum distribution of heat conductance for the fixed total heat exchanger inventory. For the fixed heat exchanger inventory  $U_T$ , that is, for the constraint of  $U_H+U_L=U_T$ , defining the distribution of heat conductance  $u=U_L/U_T$  leads to:

$$U_L=uU_T, \quad U_H=(1-u)U_T \quad (17)$$

Figure 5 shows the corresponding three-dimensional diagrams among  $\bar{E}$ ,  $P_r$  and  $u$ . In the calculation,  $k=1.4$ ,  $\tau_3=1.25$ ,  $\tau_4=1$ ,  $U_T=5\text{kW}/K$ ,  $C_L=C_H=1.0\text{kW}/K$  and  $C_{wf}=0.8\text{kW}/K$  are set. It indicates that the curve of  $\bar{E}$  versus  $u$  is parabolic-like one for a fixed pressure ratio ( $P_r$ ). There exists an optimal distribution of heat conductance ( $u_{opt,\bar{E}}$ ) corresponding to maximum dimensionless ecological function ( $\bar{E}_{max,u}$ ).

When  $C_L/C_H=1$  is satisfied, to find the maximum dimensionless ecological function ( $\bar{E}_{max,u}$ ), taking the derivatives of  $\bar{E}$  with respect to  $u$  and setting it equal to zero ( $\partial\bar{E}/\partial u=0$ ) yields  $u_{opt,\bar{E}}=0.5$  and leads to:

$$\begin{aligned} \bar{E}_{max,u} &= \frac{C_H \min I_{H1opt,\bar{E}} (1/\tau_3 - 1/P_r^n)(P_r^n - 1)}{C_H (2 - C_H \min I_{H1opt,,\bar{E}}/C_{wf})} - \frac{2\sigma}{\tau_4 C_H} \\ &= \frac{C_L \min I_{L1opt,,\bar{E}} (1/\tau_3 - 1/P_r^n)(P_r^n - 1)}{C_H (2 - C_L \min I_{L1opt,,\bar{E}}/C_{wf})} - \frac{2\sigma}{\tau_4 C_H} \end{aligned} \quad (18)$$

where

$$\sigma = 2C_H \ln \left[ \frac{1 + C_H \min I_{H1opt,\bar{E}} I_{L1opt,\bar{E}} (x/\tau_3 - 1)}{C_H C_H \min I_{H1opt,\bar{E}} (2 - C_L \min I_{L1opt,\bar{E}}/C_{wf})} \right]$$

When  $C_{wf} \neq C_H$  is satisfied,  $I_{H1opt,\bar{E}}$  and  $I_{L1opt,\bar{E}}$  are given by

$$I_{H1opt,\bar{E}} = I_{L1opt,\bar{E}} = \frac{1 - \exp[(-U_T/2C_{H\min})(1 - C_{H\min}/C_{H\max})]}{1 - (C_{H\min}/C_{H\max}) \exp[(-U_T/2C_{H\min})(1 - C_{H\min}/C_{H\max})]} \quad (19a)$$

When  $C_{wf} = C_H = C_L$  is satisfied,  $I_{H1opt,\bar{E}}$  and  $I_{L1opt,\bar{E}}$  are given by

$$I_{H1opt,\bar{E}} = I_{L1opt,\bar{E}} = \frac{1}{1 + \frac{(2C_{wf})}{(U_T)}} \quad (19b)$$

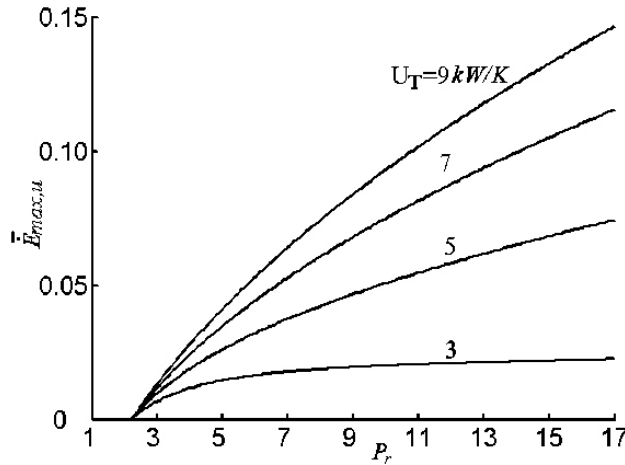


FIGURE 6. Effect of heat exchanger inventory on the maximum dimensionless ecological function vs. pressure ratio.

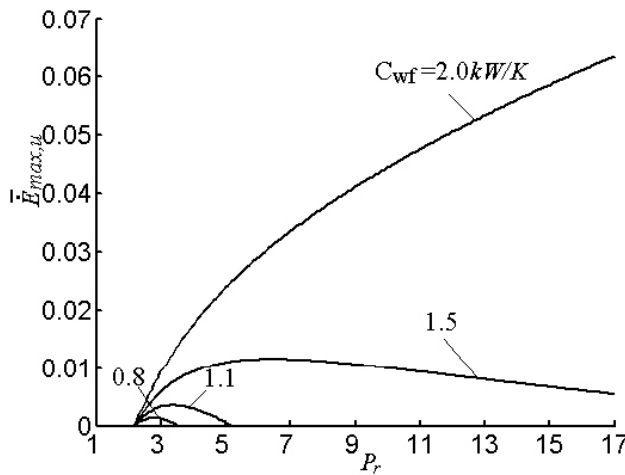


FIGURE 7. Effect of heat capacity rate of the working fluid on the maximum dimensionless ecological function vs. pressure ratio.

Figure 6 shows the effect of heat exchanger inventory ( $U_T$ ) on the maximum dimensionless ecological function ( $\dot{E}_{\max,u}$ ) versus pressure ratio  $P_r$  with  $k=1.4$ ,  $\tau_3=1.25$ ,  $\tau_4=1$ ,  $C_L = C_H = 1.0\text{ kW/K}$  and  $C_{wf} = 0.8\text{ kW/K}$ . It illustrates that  $\dot{E}_{\max,u}$  is increasing function of  $U_T$ , and it increases less if  $U_T$  gets larger. Thus, the performance of the cycle can be optimized by increasing  $U_T$  in a certain extension.

Figure 7 shows the effect of heat capacity rate of the working fluid ( $C_{wf}$ ) on the maximum dimensionless ecological function ( $\dot{E}_{\max,u}$ ) versus  $P_r$  with  $k=1.4$ ,  $U_T=5\text{ kW/K}$ ,  $C_L = C_H = 1.0\text{ kW/K}$ ,  $\tau_3=1.25$  and  $\tau_4=1$ . It indicates that the curve of  $\dot{E}_{\max,u}$  versus  $P_r$  is parabolic-like one for a smaller  $C_{wf}$ , however,  $\dot{E}_{\max,u}$  becomes to be a increasing

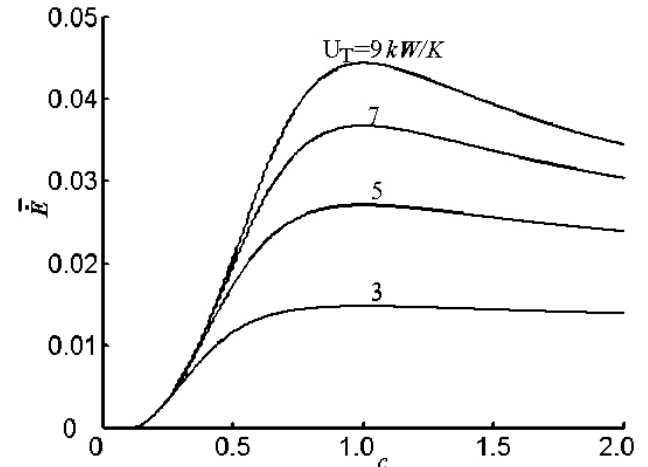


FIGURE 8. Effect of total heat exchanger inventory on the dimensionless ecological function vs. heat capacity rate matching between the working fluid and heat reservoirs.

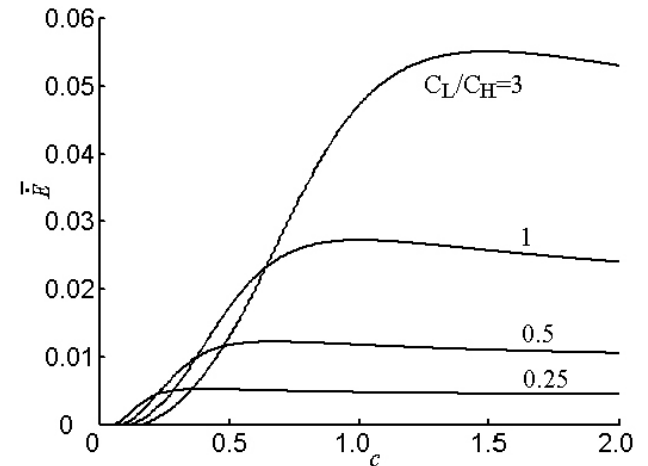


FIGURE 9. Effect of the ratio of heat reservoirs capacitance rate on the dimensionless ecological function vs. heat capacity rate matching between the working fluid and heat reservoirs.

function of  $P_r$  when  $C_{wf}$  increases to a certain value.  $\dot{E}_{\max,u}$  always increases when  $C_{wf}$  increases for a fixed pressure ratio ( $P_r$ ).

### 3.3. Optimal thermal capacity rate matching between the working fluid and heat reservoirs

The effect of thermal capacity rate matching ( $c = C_{wf}/C_H$ ) between the working fluid and the heat reservoir on the ecological function is analyzed by numerical examples. In the calculation,  $k=1.4$ ,  $C_L = 1.0 \text{ kW/K}$ ,  $u = 0.5$ ,  $P_r=5$ ,  $\tau_3=1.25$  and  $\tau_4=1$  are set.

Figure 8 shows the effect of total heat exchanger inventory ( $U_T$ ) on the dimensionless ecological function ( $\bar{E}$ ) versus thermal capacity rate matching between the working fluid and heat reservoir with  $C_L/C_H=1$ . Figure 9 shows the effect of the ratio of heat reservoir thermal capacitance rate ( $C_L/C_H$ ) on the dimensionless ecological function ( $\bar{E}$ ) versus thermal capacity rate matching between the working fluid and heat reservoir with  $U_T = 5 \text{ kW/K}$ .

The numerical examples show that the thermal capacitance rate matching ( $c$ ) between the working fluid and heat reservoir influences the ecological function obviously. The relationship is also affected by the ratio of heat reservoirs capacitance rate ( $C_L/C_H$ ). For the fixed  $C_L/C_H$ ,  $\bar{E}$  versus  $c$  is parabolic-like shaped curve. That is, there exists optimum heat capacitance rate matching between the working fluid and heat reservoir ( $c_{opt,\bar{E}}$ ) corresponding to maximum dimensionless ecological function ( $\dot{E}_{\max,c}$ ). When  $c$  varies between zero and  $c_{opt,\bar{E}}$ , the corresponding  $\bar{E}$  increases obviously as  $c$  increases. When  $c > c_{opt,\bar{E}}$  is satisfied, the corresponding  $\bar{E}$  decreases very slowly with the increasing of  $c$ .  $\dot{E}_{\max,c}$  always increases when  $U_T$  increases, and it in-

creases less if  $U_T$  gets larger. Numerical calculation shows that  $\dot{E}_{\max,c}$  and  $c_{opt,\bar{E}}$  increase when  $C_L/C_H$  increases.

## 4. Conclusion

An exergy-based ecological optimization criterion, which consists of maximizing a function representing the best compromise between the exergy output rate and exergy loss rate of a variable-temperature heat reservoir endoreversible heat pump cycle is derived. The relation among exergy-based ecological function, COP, heating load and entropy generation rate is deduced. The design parameters corresponding to the ecological optimization criterion are obtained. There exist the optimum distributions of heat conductance corresponding to the maximum ecological function, and there also exist the optimum thermal capacity rate matching between the working fluid and heat reservoir corresponding to the maximum ecological function, respectively.

The effects of various parameters, such as the temperature ratio of two heat reservoirs, the ratio of hot-side heat reservoir temperature to ambient temperature, the total heat exchanger inventory and heat capacity rate of the working fluid on the optimal exergy-based ecological performance of the cycle are analyzed using numerical examples. The analysis and optimization presented herein may provide theoretical guidelines for the design of practical air heat pump plants.

## Acknowledgements

This paper is supported by Scientific Research Common Program of Beijing Municipal Commission of Education (Project No: KM200710005034) and Program for New Century Excellent Talents in University of P. R. China (Project No: NCET-04-1006).

- 
1. G. Angelino and C. Invernizzi, *Int. J. Refrig.* **18** (1995) 272.
  2. J.S. Fleming, B.J.C. Van der Wekken, J.A. McGovern, and R.J.M. Van Gerwen, *Int. J. Energy Res.* **22** (1998) 639.
  3. J.E. Braun, P.K. Bansal, and E.A. Groll *Int. J. Refrig.* **25** (2002) 954.
  4. B. Andresen, R.S. Berry, M.J. Ondrechen, and P. Salamon, *Acc. Chem. Res.* **17** (1984) 266.
  5. Z. Yan and J.A. Chen, *J. Phys. D: Appl. Phys.* **23** (1990) 136.
  6. D.C. Agrawal and V.J. Menon, *J. Appl. Phys.* **74** (1993) 2153.
  7. J.S. Chiu, C.J. Liu, and C.K. Chen, *J. Phys. D: Appl. Phys.* **28** (1995) 1314.
  8. M. Feidt, *Thermodynamique et Optimisation Energetique des Systèmes et Procédés* (2<sup>nd</sup> Ed.). (Paris: Technique et Documentation, Lavoisier, 1996, in French).
  9. A. Bejan, *Entropy Generation Minimization*. (Boca Raton FL: CRC Press, 1996.)
  10. R.S. Berry, V.A. Kazakov, S. Sieniutycz, Z. Szwast and A.M. Tsirlin, *Thermodynamic Optimization of Finite Time Processes*. (Chichester: Wiley, 1999.)
  11. L. Chen, C. Wu, and F. Sun, *J. Non-Equilibrium Thermodyn.* **24** (1999) 327.
  12. D. Ladino-Luna, *Rev. Mex. Fis.* **48** (2002) 575.
  13. L. Chen, and F. Sun, *Advances in Finite Time Thermodynamics: Analysis and Optimization*. (New York: Nova Science Publishers, 2004).
  14. Ladino-Luna D., Paez-Hernandez R. T. Non-endoreversible Carnot refrigerator at maximum cooling power. *Revista Mexicana de Fisica*, 2005, 51(2): 54-58.
  15. G. Aragon-Gonzalez, A. Canales-Palma, A. Lenon-Galicia, and M. Musharrafie-Martinez, *Rev. Mex. Fis.* **51** (2005) 32.
  16. L. Chen, *Finite-Time Thermodynamic Analysis of Irreversible Processes and Cycles*. (Higher Education Press, Beijing, 2005.)

17. C.A. Herrera, M.E. Rosillo, and L. Castano, *Rev. Mex. Fis.* **54** (2008) 118.
18. G. Aragon-Gonzalez, A. Canales-Palma, A. Leon-Galicia, J.R. Morales-Gomez, *Brazilian J. Physics* **38** (2008) 1.
19. C. Wu, L. Chen, and F. Sun, *Energy Convers. Mangt.* **39** (1998) 445.
20. L. Chen, N. Ni, C. Wu, and F. Sun, *Int. J. Pow. Energy Sys.* **21** (2001) 105.
21. N. Ni, L. Chen, C. Wu, and F. Sun, Performance analysis for endoreversible closed regenerated Brayton heat pump cycles. *Energy Convers. Mangt.* **40** (1999) 393.
22. L. Chen, N. Ni, F. Sun, and C. Wu, *Int. J. Power Energy Sys.* **19** (1999) 231.
23. L. Chen, N. Ni, C. Wu, and F. Sun, *Int. J. Energy Res.* **23** (1999) 1039.
24. Y. Bi, L. Chen, and F. Sun, *Heating load, heating load density and COP optimizations for an endoreversible air heat pump* *Appl. Energy* **85** (2008) 607.
25. M.J. Moran, *Availability Analysis—A Guide to Efficient Energy Use*. (New York: ASME Press, 1989).
26. T.J Kotas, *The Exergy Method of Thermal Plant Analysis*. (Melbourne FL: Krieger, 1995).
27. A. Bejan, G. Tsatsaronis, and M. Moran, *Thermal Design & Optimization*. (New York: Wiley, 1996).
28. I. Dincer and Y.A. Cengel, *Energy, entropy and exergy concepts and their roles in thermal engineering*. *Entropy*, **3** (2001) 116.
29. F. Angulo-Brown, *J. Appl. Phys.* **69** (1991) 7465.
30. Z. Yan, *J. Appl. Phys.* **73** (1993) 3583.
31. L. Chen, F. Sun, and W. Chen, *J. Engng. Thermal Energy Pow.* **9** (1994) 374.
32. L. Chen, X. Zhu, F. Sun, and C. Wu, *Exergy-based ecological optimization for a generalized irreversible Carnot heat pump*. *Appl. Energy* (2007) **84** 78.
33. X. Zhu, L. Chen, F. Sun, C. Wu, *Int. J. Exergy*, (2005) **2** 423.
34. X. Zhu, L. Chen, F. Sun, and C. Wu, *J. of Energy Institute* **78** (2005) 5.
35. S.K. yagi, S.C. Kaushik, and R. Salohtra, *J. Phys. D: Appl. Phys.* **35** (2002) 2065.
36. G. Qin, M. Li, and E.X. Cheng, *Air Refrigerator*. (National Defense Industry Press, Beijing, 1980).